2nd URSI AT-RASC, Gran Canaria, 28 May – 1 June 2018

Characteristics of Medium-Scale F-region Plasma Irregularities at Equatorial and Mid Latitudes, as Observed by COSMIC Radio Occultation Receivers

C. Watson*(1) and N. Pedatella(2)

(1) University Corporation for Atmospheric Research, COSMIC Program Office, Boulder, CO, USA
(2) High Altitude Observatory, National Center for Atmospheric Research, Boulder, CO, USA

Abstract

Medium-scale ionospheric plasma irregularities are a persistent global feature of the earth's F-region ionosphere. Constellation Observing System for Meteorology, Ionosphere, and Climate (COSMIC) radio occultation (RO) measurements are well suited to address the incomplete global observational picture of irregularities, including their structure in the vertical dimension. A climatological database of ionospheric irregularities and their characteristics (e.g. magnitude, scale size, gradient, and associated scintillation) has been developed through detection of total electron content (TEC) perturbations by COSMIC precise orbit determination (POD) antennas and associated receivers of the Global Positioning System (GPS). Vertical scale sizes ranging from ~2 to 50 km were resolved from 1 Hz TEC measurements. The irregularity database will be developed into a climatological data product available to the scientific community, which will describe the global or regional occurrence and characteristics of irregularities based on user input. This paper highlights results of the initial climatological study at equatorial to mid latitudes, as well as the potential applications of the forthcoming data product. The irregularity climatology provides insight into the source and generation mechanisms of irregularities observed at particular local times and geographical regions.

1. Introduction

The focus of this study is "mesoscale" (medium-scale) ionospheric plasma irregularities in the F-region ionosphere, with vertical scale sizes in the range of ~2-50 km. The bulk of Global Navigation Satellite System (GNSS) studies have involved ground-based observations of these irregularities, which provide the high-resolution structure and propagation in the horizontal dimension [1], but miss out on critical information pertaining to their vertical structure. Global radio occultation measurements of COSMIC provide a valuable opportunity to address this observational gap, and help resolve some of the mechanisms that generate these irregularities. "Mesoscale" irregularities have been defined as ionospheric structures with scale sizes of 50-1000 km horizontally and 0.5-50 km vertically [2].

Direct energy input from the solar wind and magnetosphere, such as the precipitation of energetic particles and ultra-low frequency (ULF) geomagnetic pulsations, generate irregularities on a broad range of time and spatial scales [1]. Atmospheric gravity and acoustic waves from sources such as the solar terminator, atmospheric heating, and natural hazards (e.g. earthquakes) [3] generate traveling ionospheric disturbances (TIDs) globally on a daily basis. Internal plasma instabilities, such as gradient-drift (GDI), Rayleigh-Taylor (RTI), or Perkins instability can also generate or amplify these medium-scale disturbances [2].

Given the global observational coverage of radio occultation measurements, RO studies of medium-scale plasma structures have a high potential benefit, but are currently very limited. One study used COSMIC TEC measurements to observe medium-scale F-region irregularities associated with the Tohoku earthquake off the coast of Japan in 2011 [4]. COSMIC measurements have also been used to investigate the global climatology of E and F-region amplitude scintillation and small-scale sporadic-E irregularities [5].

2. Data and Analysis

Radio occultation TEC measurements of the COSMIC POD GPS receivers and associated antennas are used for irregularity detection. The absolute TEC measurements are contained in podTec files in the COSMIC Data Analysis and Archive Center (CDAAC: http://cdaac-www.cosmic.ucar.edu) database, and are available at a temporal resolution of 1 Hz. TEC is electron volume density integrated along the GPS satellite-to-receiver ray path, which is calculated by taking the differential phase of L1 and L2 signals at the receiver. One TEC unit (TECU) is defined as 10^{16} electrons per square meter. Only TEC during occultation events was analyzed in this study, for tangent point altitudes of 120-720 km. This altitude range was selected in order to avoid effects of sporadic-E, which typically occurs below 110 km, and artificial TEC perturbations due to the data processing often observed near COSMIC satellite altitude (~800 km).

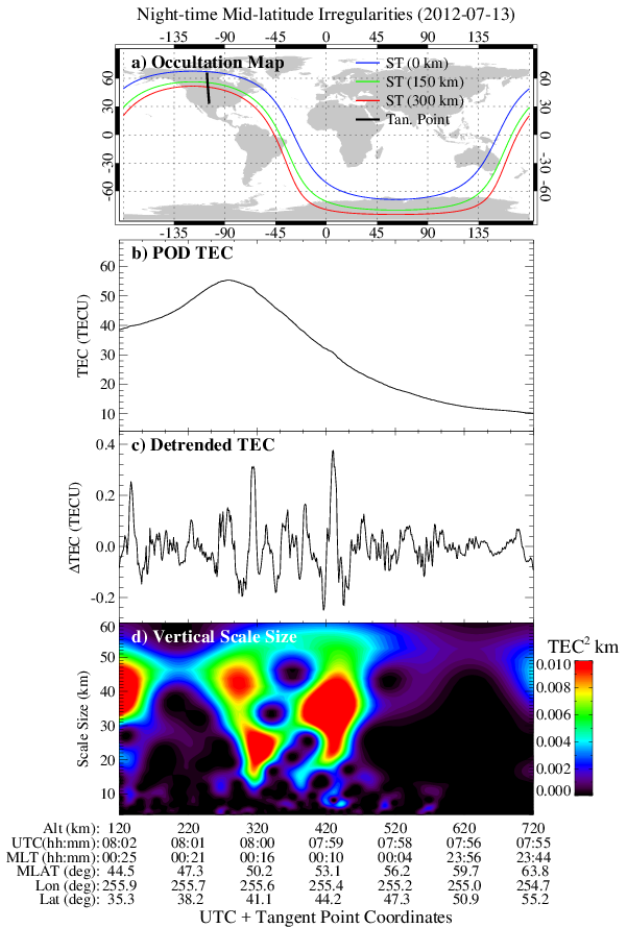

Figure 1. Example of irregularities observed during a COSMIC occultation event, showing (a) coordinates of the occultation tangent point and solar terminator (ST), (b) absolute TEC from the COSMIC POD antenna, (c) detrended TEC, and (d) dynamic power spectrum of the TEC showing irregularity scale size.

An example of TEC variations associated with medium-scale irregularities is shown in Figures 1. Figure panels show (a) RO tangent point coordinates, (b) absolute TEC, (c) detrended TEC, and (d) the TEC dynamic power spectrum. In order reveal the "medium-scale" perturbations, the TEC is detrended (Figure 1c) with a third-order high-pass Butterworth filter, which removes TEC variations with vertical scales larger than ~50 km. Individual spectral components in the dynamic power spectra (Figure 1d) that correspond to TEC perturbations larger than 0.1 TECU are designated as individual irregularities, with characteristics such as scale size, spectral power, perturbation amplitude, vertical TEC gradient, and rate of TEC (ROTI) index recorded for each observed irregularity. Parameters such as amplitude scintillation (S4) index (from COSMIC scnLv1 files), solar wind measurements, f10.7 solar flux, and geomagnetic indices are also recorded and stored in a database for future analysis.

Results here focus on equatorial to mid-latitude irregularities, while the characteristics of high-latitude irregularities will be presented in a future study. Four years of COSMIC data was analyzed: two near solar minimum (2008-2009) and two during the ascending phase of solar cycle 24 (2012-2013).

3. Global Irregularity Occurrence Rate

Figure 2 shows the occurrence rate of irregularities observed in the topside F-region (420-720 km) around (a) December solstice and (b) June solstice, for all four years of analysis. The magnetic dip equator and ±25° magnetic latitudes (MLAT) are indicated by a solid and dashed white line, respectively. Irregularities are persistently observed at high latitudes (up to 90% occurrence rate), as indicated by the white color in the contour maps. At mid and equatorial latitudes, irregularities tend to occur in seasonally-dependent localized regions. Around December Solstice, topside equatorial irregularities are mainly observed in the American sector (up to 28% occurrence), in the region corresponding closely to the South Atlantic Anomaly (SAA), with lower occurrence rates extending over the South Pacific towards Asia in southern at -10° to -25° MLAT. Around June solstice, peak equatorial occurrence is over Africa (23%) and in the mid-Pacific (19%). Equatorial occurrence rates around March and September equinox (not shown) are more longitudinally uniform, with highest occurrence (18-20%) over Africa. These longitudinal and seasonal trends closely match climatology of equatorial plasma bubbles (EPB) observed in the evening local time sector by Defense Meteorological Satellite Program (DMSP) satellites at ~840 km altitude [6], as well as the COSMIC equatorial scintillation climatology [5], although it is not clear how or if medium-scale structures relate to the smaller scale scintillation-producing structures. Factors that impact the Rayleigh-Taylor instability (RTI) growth rate, such as geomagnetic field strength and ionospheric Pederson conductivity, may influence the seasonal and longitudinal dependence of equatorial irregularity occurrence in Figure 2.

At mid-latitudes (about ±25° to ±55° MLAT), peak occurrence is observed near the eastern United States and southern tip of South America around December solstice (19-20%), and in the north-western Pacific and Oceania region around June solstice (20-23%). Mid-latitude occurrence is below 8% in all longitudinal regions around the two equinoxes. Previous climatological results based on in-situ plasma irregularity observations of ROCSAT-1 (600 km) and CHAMP (300-450 km) [7] have shown similar seasonal and longitudinal trends, which has been attributed to medium-scale travelling ionospheric disturbances (MSTIDs) and mid-latitude spread-F (MSF) irregularities.

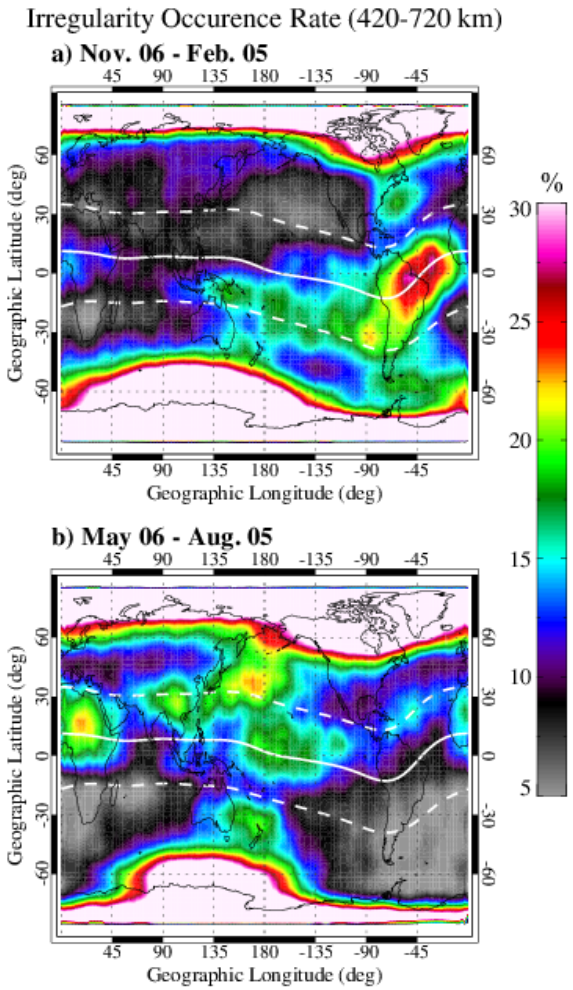

Figure 2. Occurrence rate of irregularities observed around (a) December and (b) June solstice, in the topside F-region (420-720 km).

4. Mid-Latitude Irregularity Characteristics

Figure 3 shows the occurrence rate of mid-latitude irregularities in the northern hemisphere (25° to 50°) for both solar quiet (left column) and solar active (right column) years. Occurrence is plotted with respect to tangent point altitude and MLT, and is organized vertically according to season. Irregularities are generally confined to lower altitudes (below 300 km) during the day, but are frequently observed at higher altitudes at night. High occurrence rates of 75-85% in the evening and 55-80% in the morning indicate irregularities possibility associated with the solar terminator.

In general, irregularities are more commonly observed at night compared to the day, particularly at high altitudes (>300 km). Nighttime occurrence rates peak around midnight, with higher occurrence in the summer hemisphere compared to the winter. These trends are in general agreement with previous MSTID and MSF climatology [7]. A significant solar cycle dependence is also evident, with higher nighttime occurrence during solar active years around June solstice and the two equinoxes. This trend contradicts previous mid-latitude irregularity climatology, where studies based on in-situ observations reported a decrease in MSTID and MSF occurrence with increased solar activity [7]. However, also note the apparent anti-correlation of irregularity occurrence with solar activity around December solstice. These solar cycle trends, and apparent contradiction with previous results, will be addressed further.

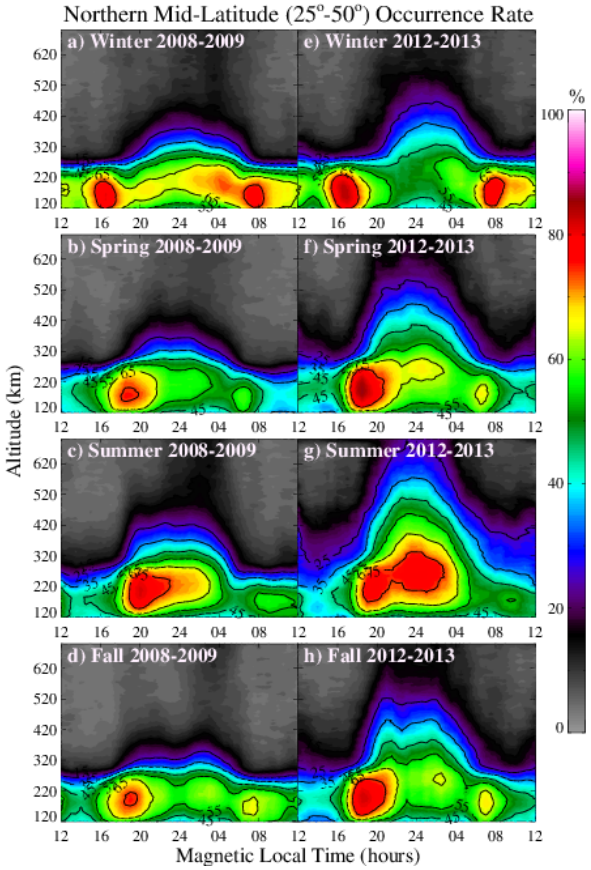

Figure 3. Occurrence rate of northern mid-latitude irregularities observed organized according to solar cycle phase (horizontally) and season (vertically).

5. Equatorial Irregularity Characteristics

Figure 4 shows the occurrence rate (top row), mean amplitude (middle), and mean vertical scale size (bottom) of equatorial (-10°-10° MLAT) irregularities, for both solar quiet (left column) and solar active (right column) years near September equinox. Following the well-known pattern of equatorial "spread-F" irregularities, high occurrence is generally observed starting around sunset, extending into the early morning hours. The most intense irregularities are observed around 20:00-24:00 MLT, and correspond to a decrease in the average irregularity scale-size. An interesting feature is the significant increase in irregularity occurrence and intensity around 20:00-24:00 MLT at high altitudes in solar active years, with peak average intensity observed around 400-440 km altitude (1.6-1.8 TECU). This solar cycle trend may be related to higher F-layer altitudes and vertical density gradients during solar active years [8], and a corresponding larger RTI growth rate under such conditions [9].

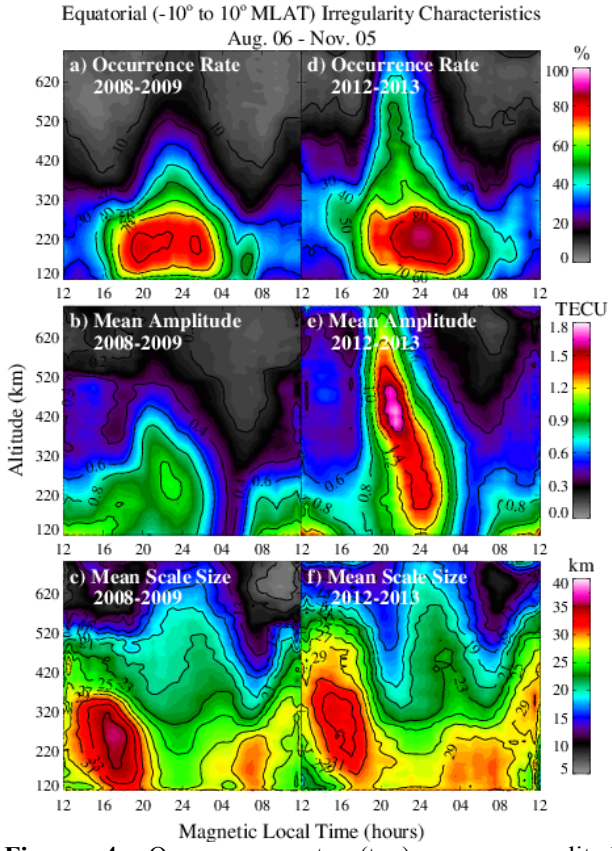

Figure 4. Occurrence rate (top), mean amplitude (middle), and mean scale size (bottom) of equatorial irregularities, organized according to solar cycle phase (horizontally).

6. Conclusions and Future Work

The COSMIC RO TEC measurements provide a global picture of medium-scale (2-50 km) F-region irregularities, and allow for investigation of the characteristics of irregularities from a new and unique perspective. We are currently working to compile an irregularity database that includes the entire COSMIC dataset and data from other RO missions, and are developing a climatological data product that will be available to the scientific community. Ongoing studies include investigation of the characteristics of irregularities during geomagnetic storms, magnetospheric substorms, sudden stratospheric warming events, and at high latitudes. We are also developing techniques to quantify uncertainties in climatological maps due to the assumption of irregularity localization at the RO tangent point.

7. Acknowledgements

Research funding is from the National Science Foundation (NSF) and National Aeronautics and Space Administration (NASA), via the University Corporation for Atmospheric Research (UCAR). Solar wind data was obtained from the OMNI database on CDAWeb (http://cdaweb.gsfc.nasa.gov/). Geomagnetic indices are from the National Geophysical Data Center (NGDC) of the National Oceanic and Atmospheric Administration (NOAA). Magnetic field data is from The International Geomagnetic Reference Field (IGRF), generated by open-source software provided by the International Associated of Geomagnetism and Aeronomy (IAGA-https://www.ngdc.noaa.gov/IAGA/vmod/igrf.html).

8. References

1. C. Watson, P. T. Jayachandran, H. J. Singer, R. J. Redmon, and D. Danskin, "GPS TEC response to Pc4 "giant pulsations"," *J. Geophys. Res. Space Physics*, **121**, 2016, doi:10.1002/2015JA022253.

2. M. C. Kelley, "The Earth's Ionosphere: Plasma Physics and Electrodynamics," *Academic Press, Inc.,* 1989, San Diego, California, USA

3. A. Komjathy, Y. -M. Yang, X. Meng, O. Verkhoglyadova, A. J. Mannucci, and R. B. Langley, "Review and perspectives: Understanding natural-hazards-generated ionospheric perturbations using GPS measurements and coupled modeling," *Radio Sci.*, **51**, 2016, 951–961, doi:10.1002/2015RS005910.

4. P. Coïsson, P. Lognonné, D. Walwer, and L. M. Rolland, "First tsunami gravity wave detection in ionospheric radio occultation data," *Earth and Space Science*, **2**, 2015, 125–133. doi:10.1002/2014EA000054.

5. B. A. Carter, K. Zhang, R. Norman, V. V. Kumar, and S. Kumar, "On the occurrence of equatorial F-region irregularities during solar minimum using radio occultation measurements," *J. Geophys. Res. Space Physics*, **118**, 2013, 892–904, doi:10.1002/jgra.50089.

6. W. J. Burke, C. Y. Huang, L. C. Gentile, and L. Bauer, "Seasonal-longitudinal variability of equatorial plasma bubbles," *Ann. Geophys.,* **22**, 2004, 3089-3098, https://doi.org/10.5194/angeo-22-3089-2004.

7. J. Park, H. Lühr, K. W. Min, and J.-J. Lee, "Plasma density undulations in the nighttime mid-latitude F-region as observed by CHAMP, KOMPSAT-1, and DMSP F15," *J. Atmos. Terr. Phys.,* **72**(2-3), 2010, 183-192, doi:10.1016/j.jastp.2009.11.007.

8. B. O. Adebesin, B. J. Adekoya, S. O. Ikubanni, S. J. Adebiyi, O. A. Adebesin, B. W. Joshua., and K. O. Olonade, "Ionospheric foF2 morphology and response of F2 layer height over Jicamarca during different solar epochs and comparison with IRI-2012 model," *Journal of Earth System Science,* **123**(4), 2014, 751-765, doi:10.1007/s12040-014-0435-y.

9. D. T. Farley, B. B. Balsey, R. F. Woodman, and J. P. McClure, "Equatorial spread *F*: Implications of VHF radar observations," *J. Geophys. Res.*, **75**(34), 1970, 7199–7216, doi:10.1029/JA075i034p07199.